JOC The Journal of Organic Chemistry

Article

pubs.acs.org/joc

DFT Study of the Mechanism and Stereochemistry of the Rh(I)-Catalyzed Diels–Alder Reactions between Electronically Neutral Dienes and Dienophiles

Wei Liao and Zhi-Xiang Yu*

Beijing National Laboratory for Molecular Sciences (BNLMS), Key Laboratory of Bioorganic Chemistry and Molecular Engineering of Ministry of Education, College of Chemistry, Peking University, Beijing 100871, China

Supporting Information

ABSTRACT: Diels–Alder reaction between electronically neutral dienes and dienophiles is usually sluggish under thermal conditions and has to be catalyzed by transition metal catalysts. We report here our DFT study of the mechanism and stereochemistry of the Rh-catalyzed Diels–Alder reaction between electronically neutral dienes and dienophiles (alkenes and alkynes), finding that this reaction includes a reaction sequence of oxidative cyclization between diene and alkene/alkyne and a reductive elimination step. The alkyne's oxidative cyclization is much faster than alkene's due to the additional coordination of alkyne to the Rh center in the oxidative cyclization transition state. For both intermolecular and intramolecular reactions, the reductive elimination step in the catalytic cycle is rate-determining. The different reactivity of ene-diene and yne-diene substrates can be rationalized by the model that reductive elimination to form a $C(sp^2)-C(sp^3)$ bond is easier than that for the formation of a $C(sp^3)-C(sp^3)$ bond, due to the additional coordination of the double bond to the Rh center in the transition state in the former. We also uncovered the reasons for the high *para*-selectivity of the intermolecular Diels–Alder reaction of dienes and alkynes. In addition, DFT calculations aiming to understand the high diastereoselectivity of an intramolecular [4 + 2] reaction of ene-dienes with substituents adjacent to the diene and ene moieties of the substrates found that the substituents in the substrates favor staying away from the Rh center in the oxidative cyclization transition states. This preference leads to the generation of the final [4 + 2] products with the substituents and the bridgehead hydrogen atoms in a *cis*-configuration.

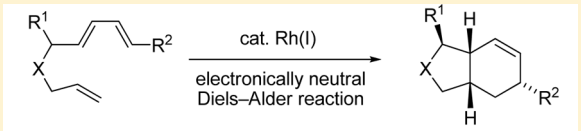

DFT Understanding of Reaction Mechanism and Stereochemistry

1. INTRODUCTION

Diels–Alder (D–A) reaction is considered to be one of the most efficient reactions to construct six-membered rings due to its one-step formation of two bonds and up to four stereocenters.[1] The D–A reactions can be divided into normal-, inverse-, and neutral-electron-demanding D–A reactions, according to the electron flow direction in their [4 + 2] transition states, either from dienes to dienophiles (normal-electron-demanding) or from dienophiles to dienes (inverse-electron-demanding), or both dienes and dienophiles can be an electron donor and an electron acceptor (neutral-electron-demanding). The normal-electron-demanding D–A reactions usually have the following requirements: the used dienophiles have electron-withdrawing groups (EWGs) to lower their LUMO energies, while the used dienes have electron-donating groups (EDGs) so that their HOMO energies can be increased.[2] When the normal-electron-demanding D–A reactions cannot be carried out thermally, Lewis acids or Brønsted acids, which can further lower the LUMO energies of dienophiles through coordination of Lewis acid to the dienophile, can be used as catalysts to speed up the reactions.[3]

The D–A reactions between electronically neutral dienes and dienophiles, neither of which has EDGs or EWGs, are very sluggish or impossible if these reactions were carried out thermally, due to the high activation barriers of these reactions.[4] For example, activation enthalpies and Gibbs activation free energies computed at the B3LYP/6-31G(d) level are 23.2 and 36.2 kcal/mol for the Diels–Alder reaction between butadiene and ethylene and 22.7 and 34.1 kcal/mol for the Diels–Alder reaction between butadiene and acetylene.[5] The experimentally measured activation energies are about 25–27 kcal/mol for the Diels–Alder reaction between butadiene and ethylene.[6] The D–A reactions between electronically neutral dienes and dienophiles (abbreviated here as ENDA reactions) cannot be catalyzed by Lewis acids or Brønsted acids because of no coordination sites of dienes and dienophiles. Fortunately, the ENDA reactions can be catalyzed by transition metal complexes through a different reaction mechanism involving metallacycle intermediates (Figure 1).[7] Two pathways for the metal-catalyzed ENDA reaction have been proposed. In pathway *a*, the catalytic cycle starts from the coordination of metal to diene, generating complex **I**. Then complex **I** undergoes oxidative cyclization to form intermediate **II** or **III**. Intermediates **II** and **III** differ from each other by the different coordination modes. Intermediate **II** has an allylic metal bond, whereas intermediate **III** is a

Special Issue: Mechanisms in Metal-Based Organic Chemistry

Received: August 3, 2014
Published: September 25, 2014

dx.doi.org/10.1021/jo5017844 | J. Org. Chem. 2014, 79, 11949–11960

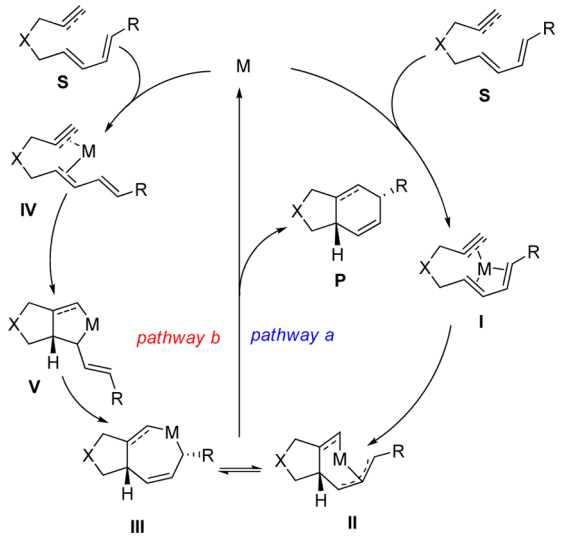

Figure 1. Generally accepted mechanism of metal-catalyzed Diels–Alder reaction between electronically neutral dienes and dienophiles.

metallacycloheptane. Finally, reductive elimination from **II** or **III** furnishes the final [4 + 2] cycloadduct **P**. Alternatively, the reaction can start from oxidative cyclization, transforming complex **IV** to intermediate **V** (pathway *b*). Then geometry reorganization takes place, converting **V** to **III**, which gives the final cycloadduct **P** via reductive elimination. Recently, Frenking and co-workers reported a DFT study of Co-catalyzed Diels–Alder reaction,[8] but Rh-catalyzed Diels–Alder reaction remains unexplored, which is the subject of the present DFT investigation.

To date, various transition metals such as Ni, Rh, Ru, Co, Au, Fe, and Pd can catalyze Diels–Alder reactions through pathways shown in Figure 1.[9] Among these transition-metal-catalyzed Diels–Alder reactions, Rh-catalyzed Diels–Alder reactions show some interesting chemistry.[10] Matsuda[11] and co-workers reported the first Rh-catalyzed intermolecular Diels–Alder reactions in 1987 using $[Rh(cod)(dppb)]PF_6$ as the catalyst, but only terminal alkynes can be used as the dienophiles in their reactions, even though their reactions had a very high *para*-selectivity (reaction a, Scheme 1). Chung[12] successfully applied disubstituted alkynes in the Diels–Alder reaction using $[Rh(cod)(naphthalene)]BF_4$ as the catalyst (reaction b, Scheme 1). Livinghouse[13] and co-workers reported the first Rh-catalyzed intramolecular [4 + 2] carbocyclizations in 1990, and since then, various Rh-catalyzed intramolecular Diels–Alder reactions have been reported.[14] Usually, the intramolecular [4 + 2] reaction of yne-diene substrates was catalyzed by cationic rhodium catalyst (reaction c, Scheme 1).[10] The intramolecular [4 + 2] reaction of ene-diene substrates can be catalyzed by either a neutral rhodium catalyst (reaction d, Scheme 1) or a cationic rhodium catalyst (reaction e, Scheme 1).[15] For the asymmetric intramolecular Diels–Alder reactions, cationic rhodium catalysts were widely used.[16] There are some features for Rh-catalyzed Diels–Alder reactions: (1) When *meta*- and *para*-products are both possible, *para*-products are favored in most cases (reactions a and b, Scheme 1).[11,12] (2) Usually, ene-diene substrates react slower than yne-diene substrates (reactions c–e, Scheme 1).[10] (3) Excellent diastereoselectivity was obtained for substrates with substituents adjacent to either the ene or diene moiety (reactions d and f).[13b] These high regioselectivities and stereoselectivities are very important for both methodology development and

Scheme 1

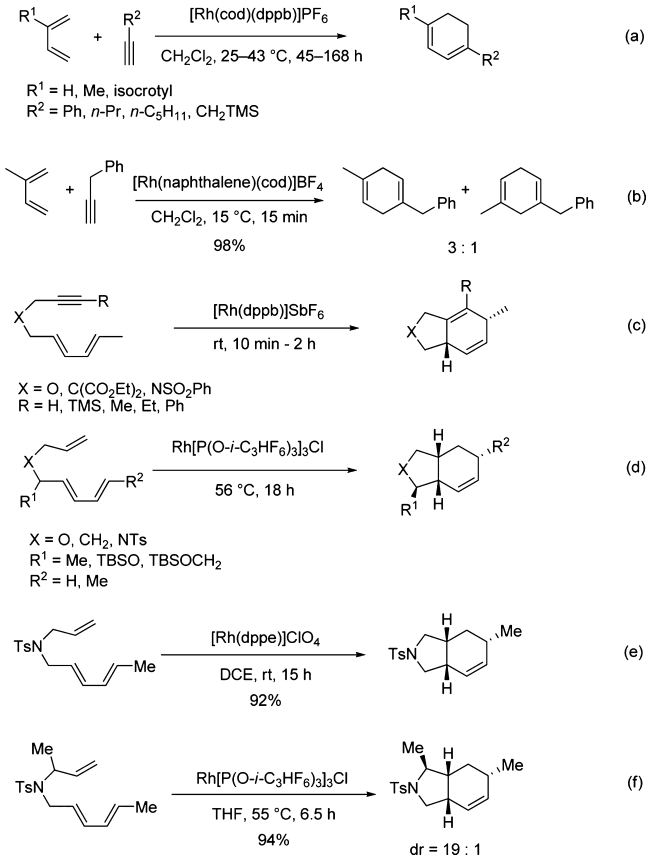

application in synthesis. However, to the best of our knowledge, there is no detailed mechanistic study using DFT calculations for the Rh-catalyzed Diels–Alder reactions. Here, we report our DFT study of Rh-catalyzed Diels–Alder reactions to understand the reaction mechanism and the regio- and stereochemistries involved.

2. COMPUTATIONAL METHODS

All calculations were performed with the Gaussian 09 program.[17] Density functional theory (DFT)[18] calculations using the B3LYP[19] functional were used to locate all the stationary points involved. The 6-31G(d)[20] basis set is applied for all elements except Rh, which uses the LANL2DZ[21] pseudopotential and basis set (for more discussion of computational methods, see the Supporting Information). This method was successfully applied to predict structures and understand reaction mechanisms for reactions of rhodium(I) complexes and many Rh-catalyzed cycloadditions.[22] Frequency calculations at the same level have been performed to confirm each stationary point to be either a minimum or a transition structure. Intrinsic reaction coordinate (IRC)[23] calculations were carried out to confirm the connection of each transition state to its corresponding reactant and product. The reported energies in the text are Gibbs free energies (ΔG) and enthalpies (ΔH), all in the gas phase at 298 K. Calculations using the M06 method to include dispersion energies showed that both B3LYP and M06 methods gave similar energy surfaces (see the Supporting Information for details), and therefore, we report our B3LYP results here. We have also computed the solvent effects and found that the conclusions obtained from the gas phase calculations do not change (see the Supporting Information). Therefore, all discussed energies in this paper refer to the Gibbs free energies in the gas phase. To simplify the calculations, we used $Rh(PMe_3)_2^+$ to model the cationic catalyst and $Rh(PMe_3)Cl$ to model the neutral catalyst. All figures of structures were prepared using CYLView.[24]

dx.doi.org/10.1021/jo5017844 | J. Org. Chem. 2014, 79, 11949–11960

3. RESULTS AND DISCUSSION

3.1. Rh-Catalyzed Intermolecular [4 + 2] Cycloaddition between Butadiene and Acetylene. In this part, we will introduce the mechanism of cationic Rh(I)-catalyzed Diels–Alder reaction between butadiene and acetylene (reaction 1, Scheme 2). Then we report our understanding of the *para*-

Scheme 2

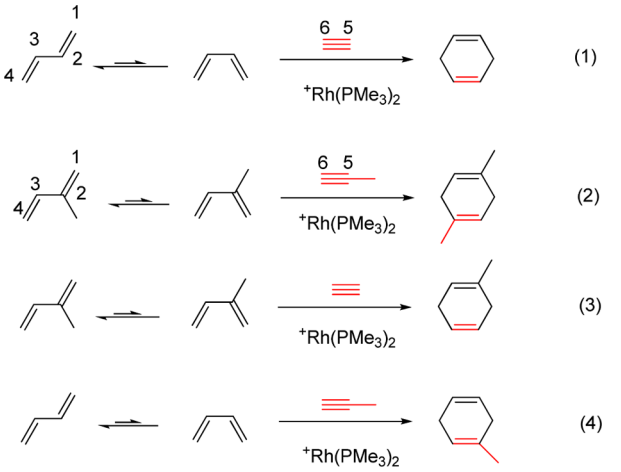

selectivity in reaction 2. Because both diene and dienophile in reaction 2 have the methyl substituents, we first investigated model reactions 3 and 4, which provided information about how the substituent in diene and dienophile affects the reaction pathway, respectively. This information can subsequently be used to analyze the regiochemistry in reaction 2 with the methyl substituents in both the diene and dienophile.

3.1.1. Mechanism of Reaction 1. The catalytic cycle of reaction 1 starts from catalyst transfer between Rh product complex **5**, which is generated in the previous catalytic cycle, and the substrate *s-trans*-butadiene **1** (Figure 2). This process releases the Diels–Alder product, cyclohexadiene **6**, together with complex **2** for the next catalytic cycle. Calculations indicated that this ligand exchange process is slightly endergonic by 2.0 kcal/mol in the gas phase. Complex **2** is a 16-e species in which *s-cis*-butadiene acts as a η^4 ligand in a symmetric pattern. The

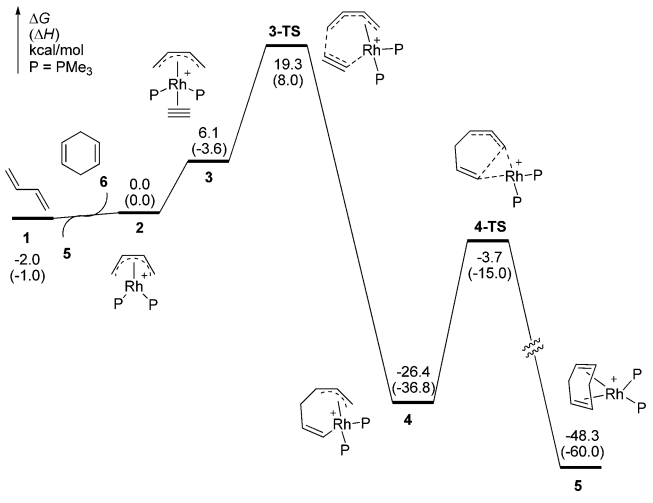

Figure 2. DFT-computed potential energy surface of Rh-catalyzed [4 + 2] reaction of butadiene and acetylene.

coordination of acetylene to complex **2** gives an 18-e species **3**, which is less stable than complex **2** by 6.1 kcal/mol. Then complex **3** undergoes oxidative cyclization to produce intermediate **4** via transition state **3-TS**. The oxidative cyclization step requires an activation free energy of 19.3 kcal/mol and is exergonic by 26.4 kcal/mol. The Rh–C5 bond in **3-TS** has been formed with a bond distance of 2.10 Å, whereas the C1–C6 bond is forming with a bond distance of 2.15 Å (Figure 3). The C2, C3, and C4 atoms act as an η^3 ligand in complex **4**. Complex **4** can undergo reductive elimination, giving complex **5** with an activation free energy of 22.7 kcal/mol (via **4-TS**), and this step is exergonic by 21.9 kcal/mol. The two C=C bonds coordinate to the Rh center in a symmetric manner in complex **5**, in which the distances between Rh and the alkene parts of the final [4 + 2] cycloadduct are both 2.32 Å.

The potential energy surface in Figure 2 shows that, in the Rh-catalyzed D–A reaction of butadiene and acetylene, the oxidative cyclization step is irreversible and the rate-determining step of the catalytic cycle is the reductive elimination step, which requires an activation free energy of 22.7 kcal/mol (23.8 kcal/mol in terms of enthalpy), and the whole reaction is exergonic by 46.3 kcal/mol. The calculations agree with the experimental results that Rh(I)-catalyzed Diels–Alder reactions can proceed at room temperature. The DFT-computed thermal reaction between diene and acetylene without using a catalyst has an activation free energy of 34.1 kcal/mol in the gas phase (the activation enthalpy is 22.7 kcal/mol). Therefore, the Rh-catalyzed ENDA reaction shown in Figure 2 is much easier than the thermal D–A reaction and can be carried out under mild reaction conditions.[5]

In dichloromethane (DCM) solution, the DFT-computed activation free energy for the reductive elimination is 25.3 kcal/mol, about 2.6 kcal/mol higher than that in the gas phase (see the Supporting Information for details). This suggests that the cationic Rh-catalyzed D–A reaction becomes slower in solution than that in the gas phase.

Pathway *b* for reaction 1 can be ruled out due to the high activation energy required for the oxidative cyclization step (via transition state **3b-TS**), which requires an activation free energy of 24.0 kcal/mol. This is higher than **3-TS** for the irreversible oxidative cyclization step in pathway *a* by 4.7 kcal/mol (Scheme 3).

3.1.2. Understanding the para-Selectivity of Reaction 2 between Isoprene and Propyne. To understand the *para*-selectivity of reaction 2, here we first discuss the regiochemistry of model reactions 3 and 4 (Scheme 2). Both reactions 3 and 4 have two possible oxidative cyclization pathways to give the same products. Even though the two competing pathways of reactions 3 and 4 do not affect the final outcomes of the [4 + 2] reactions, information obtained from these reactions can be used to understand how the substituents in both dienes and dienophiles affect the reaction pathways. DFT-calculated energy surface of reaction 3 suggests that the oxidative cyclization step prefers to occur via the unsubstituted ene pathway, in which the oxidative cyclization uses the unsubstituted ene of the diene part (Figure 4). This pathway is favored over the substituted ene pathway by 3.2 kcal/mol. We attribute this selection to the stronger Rh–allylic interaction in **8a-TS** than that in **8b-TS**. This stronger interaction can be appreciated by the fact that **9a** is more stable than **9b** by 2.9 kcal/mol. The steric repulsion between the methyl group and the ligand in **8b-TS** is stronger than that in **8a-TS** (the distances of Ha and Hb are 2.13 Å in **8b-TS** and 2.33 Å in **8a-TS**, respectively).[25]

dx.doi.org/10.1021/jo5017844 | J. Org. Chem. 2014, 79, 11949–11960

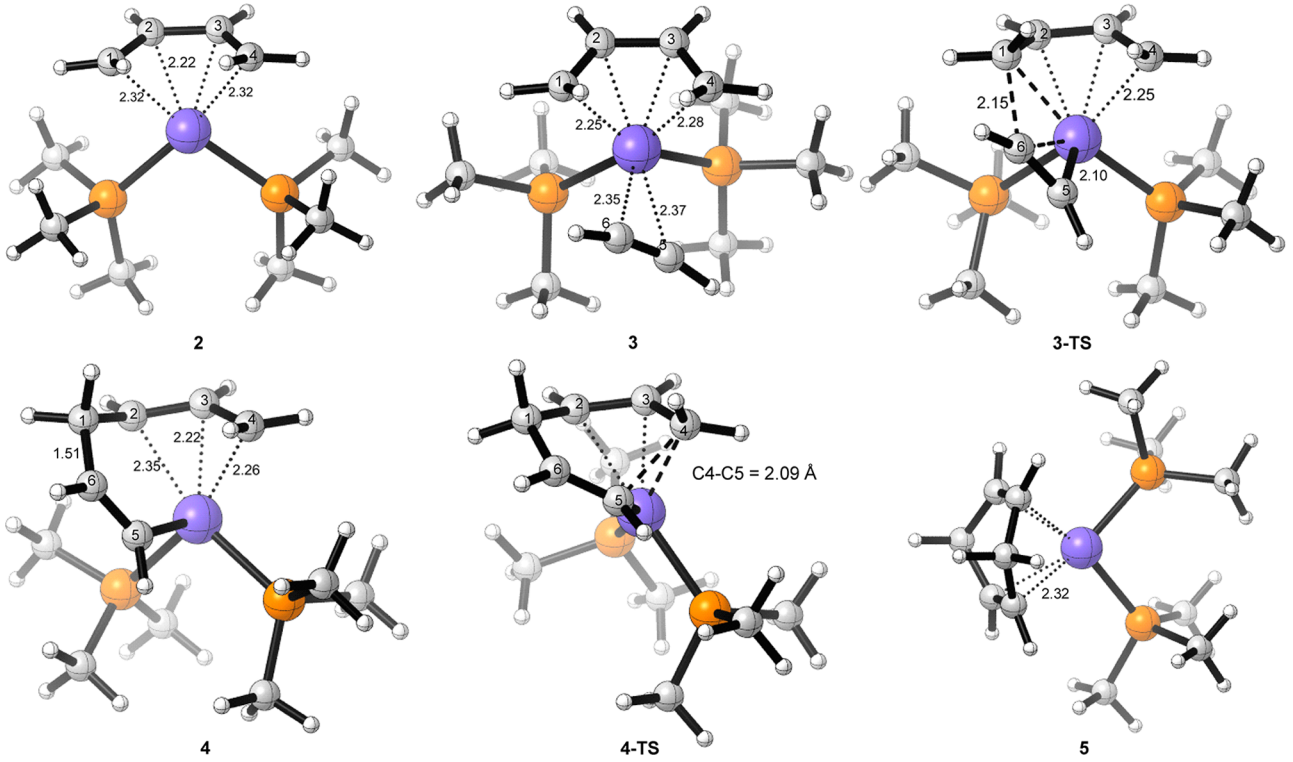

Figure 3. DFT-computed structures of intermediates and transition states for Rh-catalyzed reaction of butadiene and acetylene (reaction 1).

Scheme 3

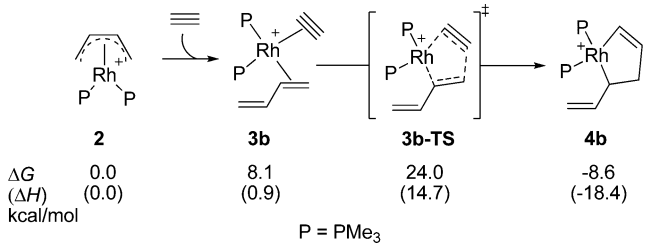

The oxidative cyclization step in reaction 4 favors the substituted yne pathway, in which the oxidative cyclization prefers to use the substituted part of the alkyne (Figure 5). The substituted yne pathway is favored over the unsubstituted yne pathway by 2.2 kcal/mol in terms of Gibbs free energy. We propose that two factors are responsible for this selectivity. One is that, in the unsubstituted yne pathway, the methyl substituent in the alkyne experiences steric repulsion from the ligand in the oxidative cyclization transition state. It was found that the methyl group in **11b-TS** points toward the ligand, whereas such repulsion is absent in the substituted yne pathway (the distance of Hb and Hc is 2.66 Å in **11a-TS**, and the distance of Hb and Hd is 2.30 Å in **11b-TS**). This disfavored steric interaction is also shown in the oxidative cyclization products, showing that **12a** is more stable than **12b**, which experiences steric repulsion between the methyl group and the ligand. In the oxidative cyclization transition states, the carbon of alkyne that is forming the C−C bond has positive charge, and consequently, the C5 atom in **11a-TS** can be stabilized by the methyl group further. In contrast, the C6 atom in **11b-TS** does not have such stabilization. Due to these two factors, reaction 4 prefers the substituted yne pathway over the unsubstituted yne pathway.

With the above understanding, we can know the encountered regiochemistry of reaction 2 (Scheme 2). This suggests that the oxidative cyclization prefers to go through the substituted yne pathway (Figure 6) for alkyne (C5 atom of **13a**) and the unsubstituted ene pathway for diene (the C4 atom of **13a**) to form a C−C bond. DFT calculations agree with this, showing that **13a-TS** is favored by 3.0 kcal/mol or more than other competing pathways, and the *para*-selectivity for the intermolecular D−A reaction can be achieved. These calculation results agree with experimental observations. We found that using the bidentate ligand of dppb, the D−A reaction also has the *para*-selectivity (see the Supporting Information for details).

3.2. Rh-Catalyzed Intramolecular [4 + 2] Cycloadditions of Butadienes with Alkynes and Alkenes. We have discussed the intermolecular Rh-catalyzed Diels−Alder reactions of butadiene and alkynes above. Here, we discuss Rh-catalyzed intramolecular Diels−Alder reactions of dienes with alkynes (section 3.2.1) and alkenes (section 3.2.2), respectively. Here we only discuss the pathway *a* because pathway *b* for both intramolecular Diels−Alder reactions is not favored (see the Supporting Information). Then the diastereoselectivity in reactions d and f (Scheme 1) will be discussed by computing the energy surfaces of all their possible pathways (sections 3.2.3 and 3.2.4).

3.2.1. Intramolecular D−A Reaction of Yne-Dienes. The computed potential energy surface of Rh-catalyzed [4 + 2] cycloaddition of yne-diene substrate **16** is given in Figure 7. The catalyst transfer step is exergonic by 2.0 kcal/mol. The coordination of the alkyne moiety of the yne-diene substrate to the rhodium center results in the increased energy by 7.0 kcal/mol. Then complex **18** undergoes oxidative cyclization through transition state **18-TS**, giving complex **19** with an activation free energy of 15.5 kcal/mol. Finally, complex **19** is converted to the final 5/6 bicyclic product **20** through the reductive elimination

dx.doi.org/10.1021/jo5017844 | J. Org. Chem. 2014, 79, 11949−11960

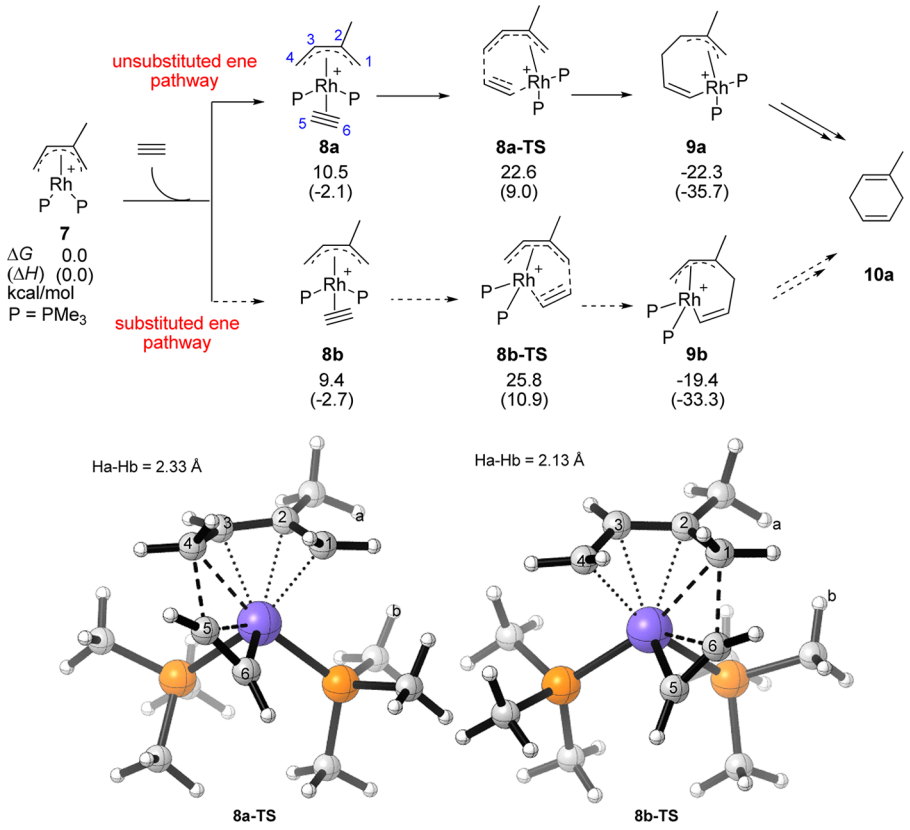

Figure 4. Calculated relative energies of Rh-catalyzed Diels–Alder reaction between isoprene and acetylene.

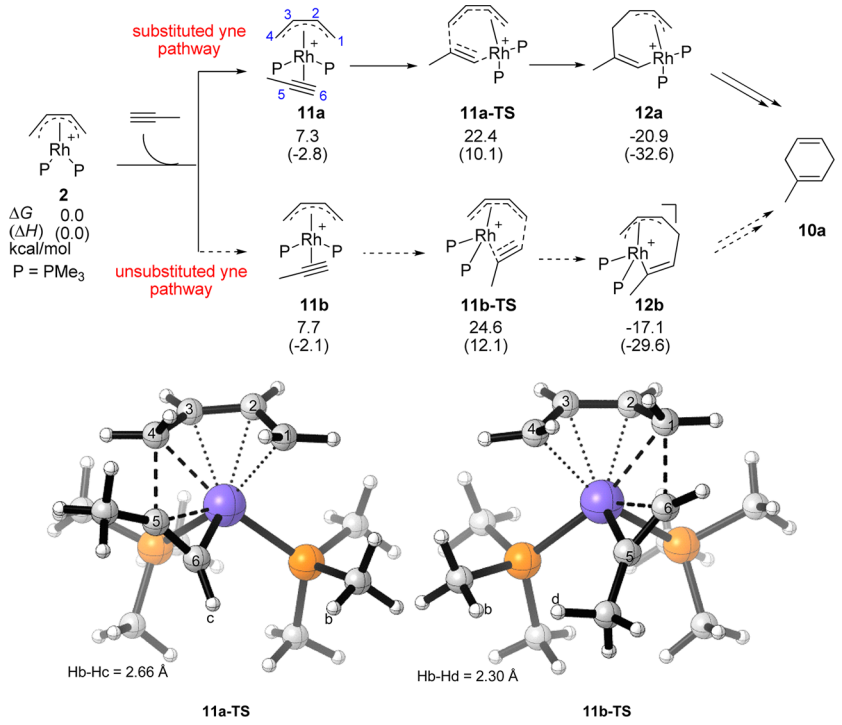

Figure 5. Calculated relative energies of Rh-catalyzed Diels–Alder reaction between butadiene and propyne.

transition state **19-TS**, which is the rate-determining step of the intramolecular reaction, with an activation free energy of 21.7 kcal/mol. The whole catalytic cycle is exergonic by 45.2 kcal/mol.

3.2.2. Intramolecular D–A Reaction of Ene-Diene and Its Stereochemistry. Experimentally, ene-diene substrates usually react slower than yne-diene substrates. To explain the different reactivities of these substrates, we computed the energy surface of the Rh-catalyzed intramolecular D–A reaction of ene-diene

dx.doi.org/10.1021/jo5017844 | J. Org. Chem. 2014, 79, 11949–11960

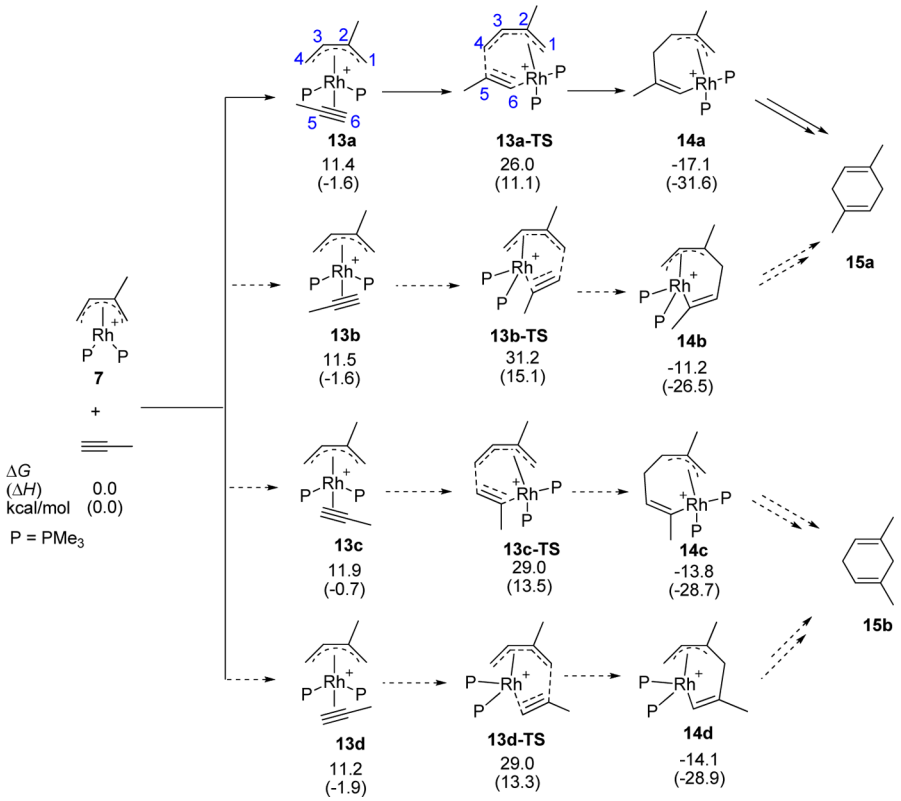

Figure 6. DFT-computed relative energies of the four different pathways for the Rh-catalyzed Diels–Alder reaction between isoprene and propyne.

substrate **22** (Figure 8; for the computed energy surface of the neutral Rh-catalyzed Diels–Alder reaction of the ene-diene substrate, see the Supporting Information). The catalytic cycle starts with the catalyst transfer step, which is exergonic by 7.8 kcal/mol and generates complex **23**. Then the alkene moiety in **23** coordinates to the rhodium center, which is followed by a *cis*-oxidative cyclization through transition state **24-TS**. The oxidative cyclization step leads to the formation of complex **25** with an activation free energy of 22.3 kcal/mol. Finally, complex **25** undergoes a reductive elimination process (via transition state **25-TS**) to generate *cis*-fused 5/6 bicyclic product **26**. It is interesting to note that the rate-determining step in the intramolecular D–A reaction of ene-diene is the reductive elimination step with an activation free energy of 23.4 kcal/mol. The whole catalytic cycle is exergonic by 26.3 kcal/mol.

Now let us compare and analyze the alkyne/alkene oxidative cyclization and reductive elimination steps in Figures 7 and 8. The energy of oxidative cyclization of alkene with diene is higher than that required for the alkyne and diene by 6.8 kcal/mol. The alkyne and alkene coordinations (forming complexes **17** and **24**) to the cationic Rh center are similar with binding energies of 7.0 and 9.1 kcal/mol, respectively. The major difference in the oxidative cyclizations for alkyne and alkene is due to the additional coordination of the alkyne moiety to the Rh center in its oxidative cyclization transition state. The alkyne's oxidative cyclization is exergonic by 21.1 kcal/mol, while the alkene's oxidative cyclization is a thermodynamically neutral process (**17** to **19** versus **23** to **25**). The coordination of alkyne to the Rh center in the transition state is still there, and consequently, its oxidative cyclization is easier than that in alkene's oxidative cyclization (in its transition state, the alkene's C=C bond becomes C–C and C–Rh single bonds). We want to point out here that the alkyne/alkene oxidative cyclization is different from the alkyne/alkene insertion in the [5 + 2] reaction of vinylcyclopropanes and alkynes/alkenes, where the alkyne/alkene insertion has very close activation energies.[22c]

The reductive elimination steps for yne-diene (forming a $C(sp^2)$–$C(sp^3)$ bond) and ene-diene (forming a $C(sp^3)$–$C(sp^3)$ bond) have similar activation free energies (21.7 vs 23.4 kcal/mol). Here we provide a model to explain why reductive elimination to form the $C(sp^3)$–$C(sp^3)$ bond is a little bit more difficult than the reductive elimination of form the $C(sp^2)$–$C(sp^3)$ bond. The reductive elimination between $C(sp^2)$ and $C(sp^3)$ atoms has an additional coordination of the vinyl group to the metal center in both the reductive elimination transition state and its product, while such coordination is absent for the reductive elimination process between two $C(sp^3)$ atoms. Consequently, reductive elimination with additional coordination is easier. This can be appreciated by the fact that reductive elimination from **19** to **20** is more exothermic than that from **25** to **26**. In complex **20**, the Rh is coordinated by two alkenes, while in **26**, the Rh is coordinated by an alkene and a C–H bond (via an agostic interaction). IRC calculations showed that such coordination assistance has been found for the reductive elimination process for **19-TS** but not for **25-TS** (see the Supporting Information).

Now we can understand why yne-diene is more reactive that ene-diene in Rh-catalyzed D–A reactions. Figures 7 and 8 suggest that the rate-determining steps for both yne-diene and ene-diene are the reductive elimination reactions, even though the alkyne's and alkene's oxidative cyclizations have different reactivities. Consequently, the overall activation free energy for yne-diene is 1.7 kcal/mol lower than that required in ene-diene's D–A reaction.

In comparison, we calculated the energy barriers of the Diels–Alder reaction of yne-diene substrate **16** and ene-diene substrate

dx.doi.org/10.1021/jo5017844 | J. Org. Chem. 2014, 79, 11949–11960

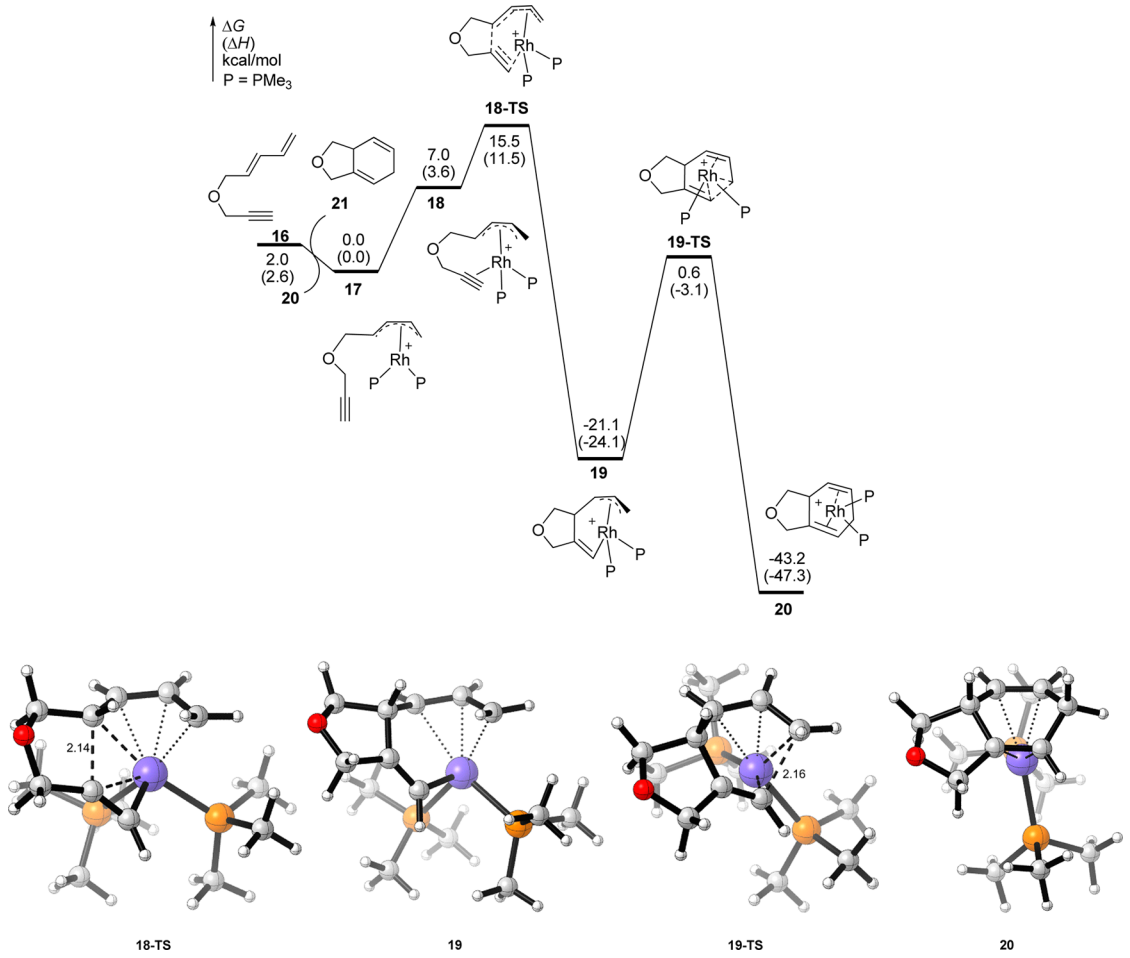

Figure 7. Potential energy surface and 3-D structures of key species of Rh-catalyzed intramolecular Diels–Alder reaction of yne-diene **16**.

22 under thermal conditions, finding that the computed activation free energies are 25.5 and 29.9 kcal/mol, respectively, for these two substrates (the activation enthalpies are 21.5 and 25.2 kcal/mol, respectively). These barriers are higher than those required for the Rh-catalyzed reactions (the computed activation free energies are 21.7 and 23.4 kcal/mol, respectively).[5] The calculation results indicated that, under rhodium catalysis conditions, the Diels–Alder reactions of yne-diene substrates and ene-diene substrates become easier.

We now discuss the stereochemistry of the Rh-catalyzed Diels–Alder reaction of ene-diene substrates. We calculated the *trans*-oxidative cyclization step and found the corresponding transition state **24b-TS** requires an activation free energy of 27.0 kcal/mol, which is higher than **24-TS** in the *cis*-oxidative cyclization pathway by 4.7 kcal/mol (Figure 9). Two factors are responsible for the higher energy of **24b-TS** with respect to *cis*-oxidative cyclization transition state **24-TS**. The first one is the torsional strain of the forming five-membered ring. In *cis*-oxidative cyclization transition state **24-TS**, the forming C2–C3–O–C4–C5 ring adopts an envelope configuration, the favored configuration for a five-membered ring, with the dihedral angles of C2–C3–O–C4 being 51.4° and C3–O–C4–C5 being −47.0°. In the *trans*-oxidative cyclization transition state **24b-TS**, the dihedral angles of C2–C3–O–C4 (−34.3°) and C3–O–C4–C5 (−11.7°) are both smaller and suffer from additional torsional strain compared to **24-TS**. Another reason is due to the steric repulsion between the hydrogen atoms (Ha and Hb) in the diene moiety (Figure 9). The distorted C2–C3–O–C4–C5 ring in **24b-TS** leads to a distance of Ha and Hb of 1.93 Å, while the distance of Ha and Hb in **24-TS** is 2.11 Å.

3.2.3. Understanding How the Substituent Adjacent to the Diene Part of the Ene-Diene Controls the Diastereoselectivity of the D–A Reaction (Reaction d in Scheme 1). Substrates with an R group near the diene or alkene moiety usually show excellent diastereoselectivity for Rh-catalyzed Diels–Alder reactions (reactions d and f, Scheme 1). Here, we will first discuss the diastereoselectivity of reaction d, and then the diastereoselectivity of reaction f will be discussed in section 3.2.4. To simplify the calculations, we chose the methyl group to represent the R group in the substrate for our calculations (Figures 10 and 11).

The complex formed by the substrate and the catalyst favors having the R group (here it is a methyl group) in the tether and the internal hydrogen atom Ha in a *cis*-configuration (**28a**), whereas complex **28b** with the Ha and R in a *trans*-configuration is higher in energy than complex **28a** by 3.0 kcal/mol. In complex **28b**, the R group has to point to the Rh catalyst, and this leads to repulsion. This repulsion between R and the Rh catalyst part can be appreciated by the torsional strain of C9–C4–C5–C6 (with a computed dihedral angle of −6.8°) in complex **28b**, where the R group (C9 atom) and C6 atom are close to being in the same plane. Alkene coordination to the Rh center in complex **28a** leads to the formation of complexes **29a** and **29b**. Complexes **29a** and **29b** are in equilibrium, and they can finally be transformed to **31a** instead of **31b** because **29a-TS** and **30a-TS** in the *cis*–*cis* pathway are both lower in energy than **29b-TS** and **30b-TS** in the *cis*–

dx.doi.org/10.1021/jo5017844 | J. Org. Chem. 2014, 79, 11949–11960

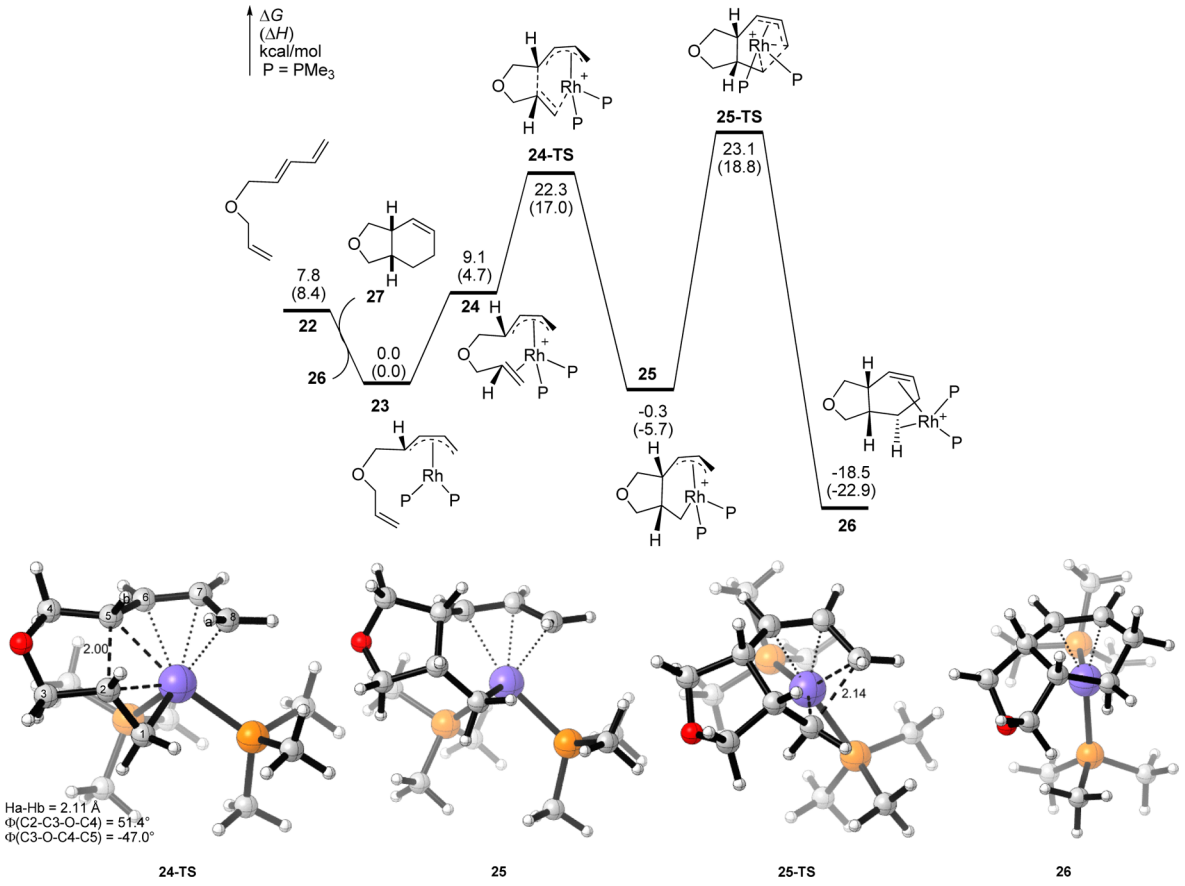

Figure 8. Potential energy surface of Rh-catalyzed intramolecular Diels–Alder reaction of ene-diene and the DFT-computed key structures.

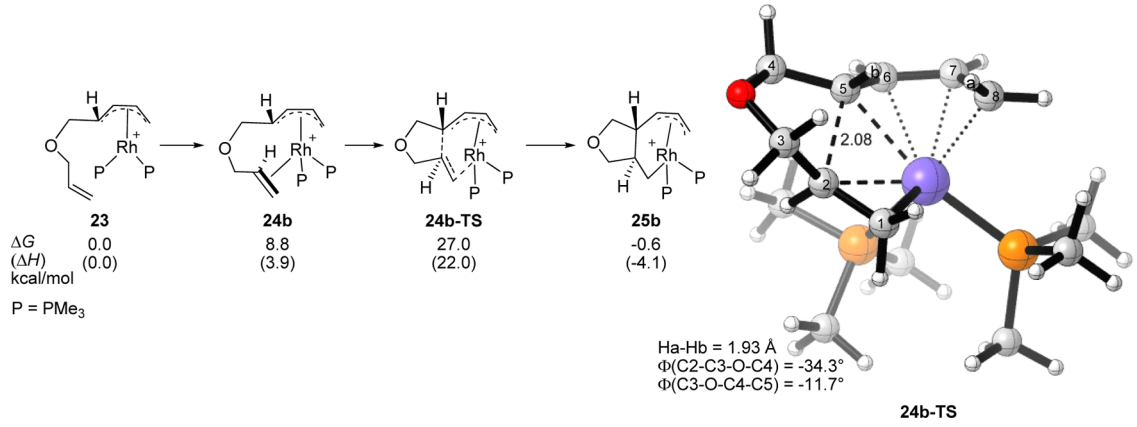

Figure 9. Calculated relative energies for the Rh-catalyzed Diels–Alder reaction of ene-diene substrate in the pathway leading to give the *trans*-fused [4 + 2] cycloadduct.

trans pathway. Therefore, the R group prefers to stay away from the Rh catalyst center and be in a *cis*-configuration with hydrogen at C5, which requires a *cis*-alkene's oxidative cyclization into the Rh–C bond (discussed in the previous part of section 3.2.2). Due to this, the R group and the bridgehead hydrogen atoms (at C5 and C2) all point to the same direction to give the favored product **31a**.

Complex **28b** also has two competing pathways to give the [4 + 2] products, **31c** and **31d**. The *trans–cis* pathway is favored over the *trans–trans* pathway, but both **29c-TS** and **29d-TS** coming from **28b** still suffer from the repulsion between the R group and the Rh catalyst center, and they are less stable than **29a-TS** in energy. Therefore, the *cis–cis* pathway is the favored one, and this pathway leads to the generation of product **31a**. A simple model to explain this stereochemistry is given in Figure 12, which stresses that the R^1 group prefers to stay away from the Rh catalyst, and this leads to the *cis*-configuration of R^1 with both the bridgehead hydrogen atoms in the final product.

3.2.4. Understanding How the Substituent Adjacent to the Ene Part of the Ene-Diene Controls the Diastereoselectivity of the D–A Reaction (Reaction f in Scheme 1). We calculated the energy surface of the ene-diene substrate with the methyl group adjacent to the ene moiety of the substrate to investigate the diastereoselectivity of reaction f shown in Scheme 1 (Figures 13 and 14). DFT calculations found that **33a-TS** is the most favored oxidative cyclization transition state compared to the other three

dx.doi.org/10.1021/jo5017844 | J. Org. Chem. 2014, 79, 11949–11960

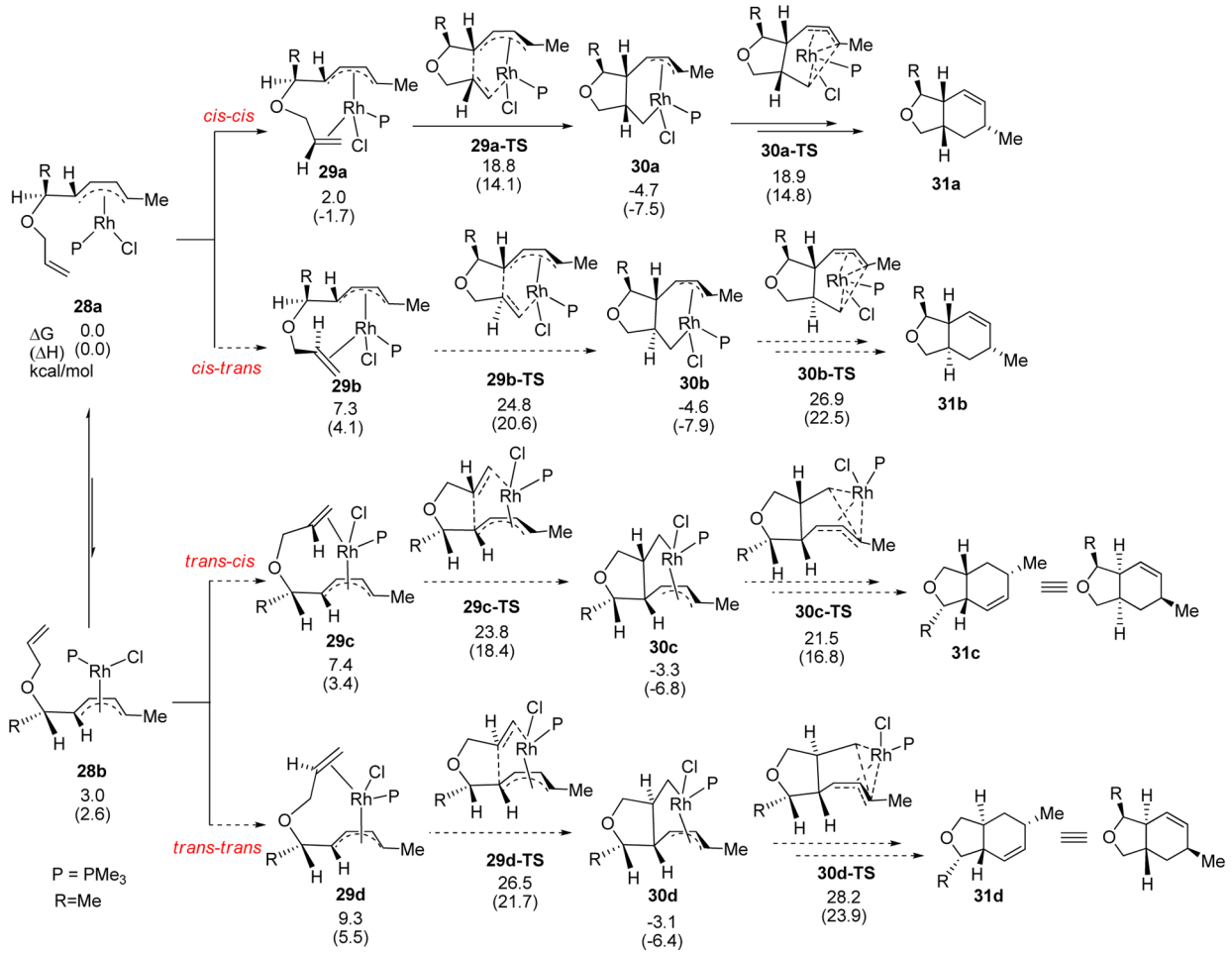

Figure 10. DFT-calculated relative energies for different pathways for ene-diene with an R substituent adjacent to the diene moiety of the substrate.

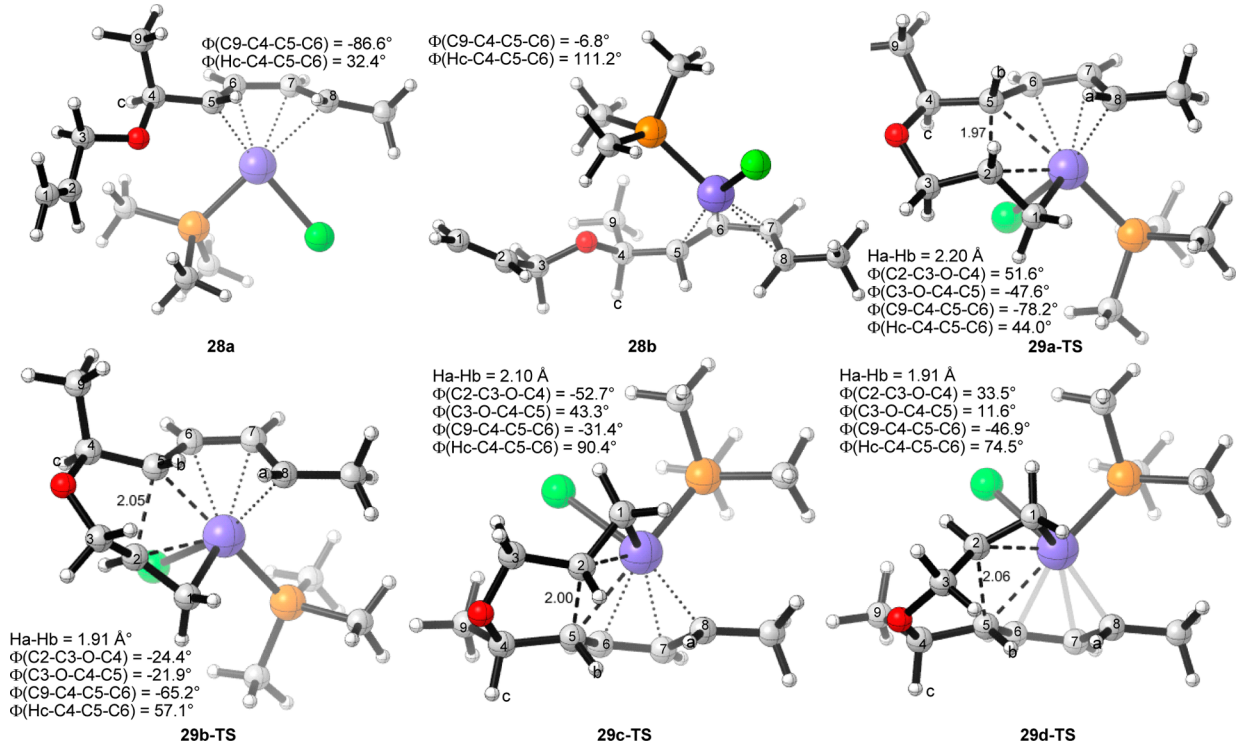

Figure 11. Optimized structures of alkene complexes and oxidative cyclization transition states for the reaction in Figure 10.

dx.doi.org/10.1021/jo5017844 | J. Org. Chem. 2014, 79, 11949−11960

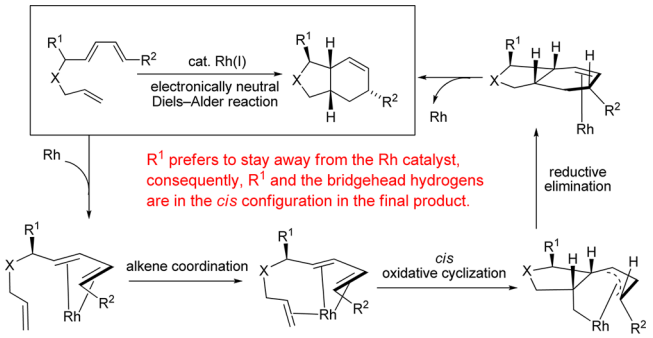

Figure 12. Proposed model to explain the diastereoselectivity of the ene-dienes with a substituent adjacent to the diene moiety of the substrates.

competing transition states of **33b-TS**, **33c-TS**, and **33d-TS**, indicating that the reaction pathway through **33a-TS** is the most favored and the corresponding product **35a** is the major product. This DFT conclusion agrees with the experimental results.

As we have discussed before, the Rh-catalyzed [4 + 2] cycloaddition of ene-diene favors having the bridgehead hydrogen atoms in a *cis*-configuration; here we will not discuss why **33b-TS** and **33d-TS** are significantly higher than **33a-TS**. We focus here on diagnosing the reason why the R group also favors being in a *cis*-configuration with the bridgehead hydrogen atoms. We found that the R group still prefers to stay away from the Rh center to avoid the repulsion, as indicated by the fact that **33c** is less stable than **33a** by 6.6 kcal/mol. The steric repulsion between R and the Rh center is also present in **33c-TS**, in which C9−C3−C2−C1 has an eclipsed conformation with a dihedral angle of 25°. In the most favored **33a-TS**, C9−C3−C2−C1 has a dihedral angle of −82.4°. Figure 15 gives a model to explain the diastereoselectivity, suggesting the substituent adjacent to the ene moiety of the substrate favors staying away from the Rh catalyst, leading to the R^1 group and the bridgehead hydrogen atoms in a *cis*-configuration.

4. CONCLUSIONS

Through DFT calculations, we have investigated the detailed mechanism of Rh-catalyzed inter- and intramolecular Diels–Alder reaction of dienes and alkynes/alkenes, which involves catalyst transfer, alkyne/alkene coordination, oxidative cyclization, and reductive elimination steps. We found that the rate-determining step is the reductive elimination step for both intramolecular D−A reactions of yne-diene and ene-diene substrates. It was found that alkyne's oxidative cyclization is much easier than alkene's oxidative cyclization, due to the additional coordination of alkyne to the Rh center, present in both the oxidative cyclization transition state and its product. Reaction between substituted diene and alkyne was also studied to reveal the *para*-selectivity, finding that both electronic and steric effects lead to this preference. In addition, we computed

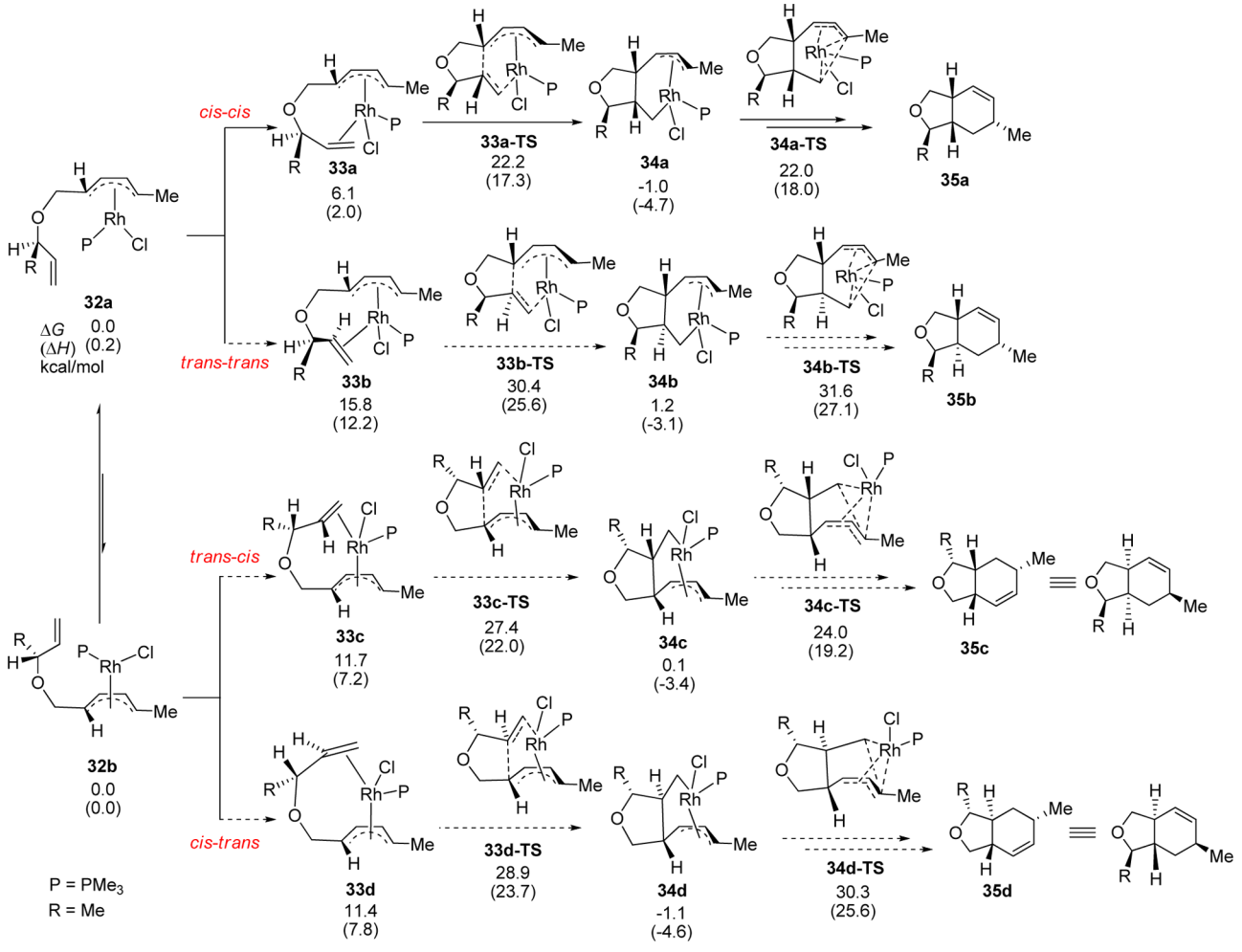

Figure 13. Calculated relative energies of ene-yne substrate with an R substituent adjacent to the ene moiety of the substrate.

dx.doi.org/10.1021/jo5017844 | J. Org. Chem. 2014, 79, 11949−11960

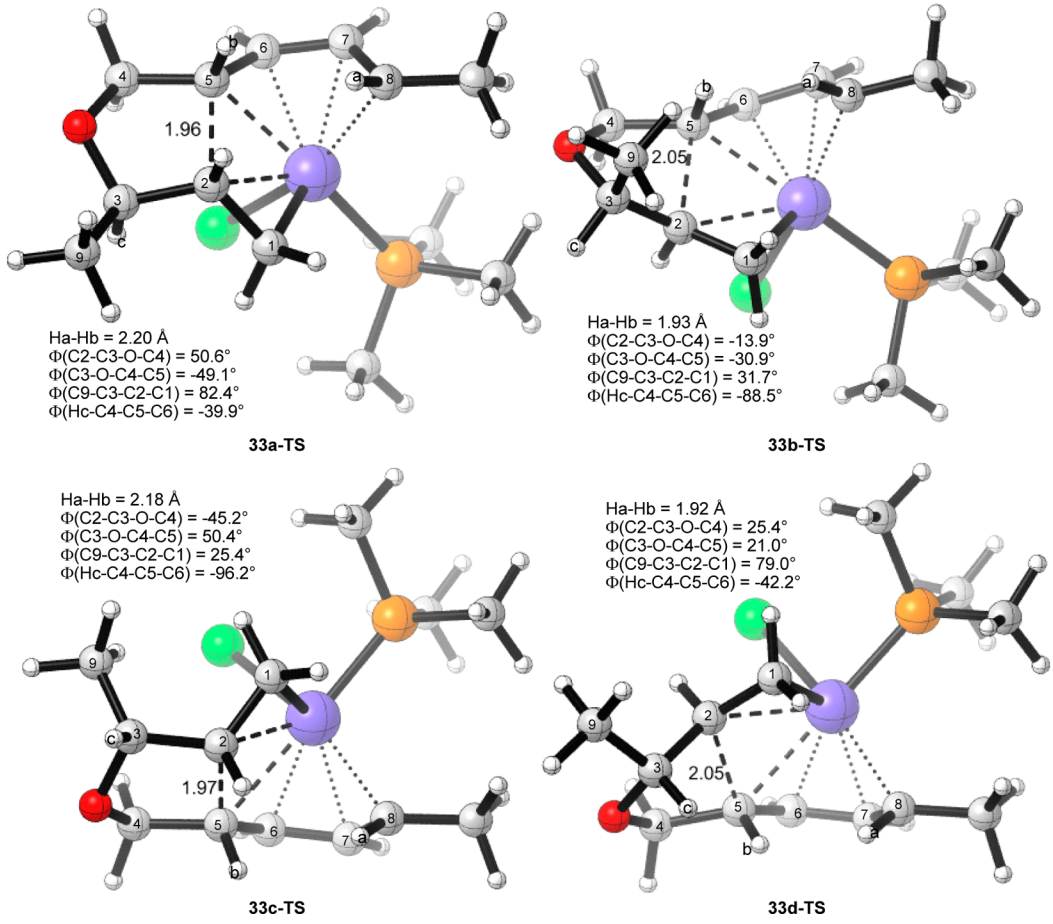

Figure 14. Optimized structures of four oxidative cyclization transition states for reaction shown in Figure 12.

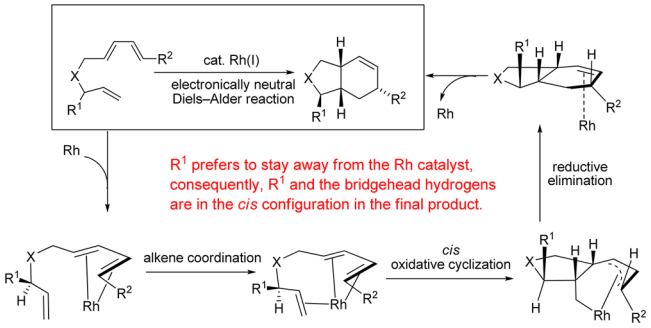

Figure 15. Proposed model to explain the diastereoselectivity of the ene-dienes with a substituent adjacent to the ene moiety of the substrates.

the potential energy surface of the intramolecular Rh-catalyzed Diels–Alder reaction of ene-dienes with substituents adjacent to the ene and diene moieties of the substrates, with the aim of uncovering the origins of the stereochemistry. DFT calculations indicated that the substituents in the ene-diene substrates favor staying away from the Rh catalyst center in the oxidative cyclization transition states, and consequently, [4 + 2] cycloadducts with the substituents the bridgehead hydrogen atoms in a *cis*-configuration were generated.

■ ASSOCIATED CONTENT

Ⓢ Supporting Information

Full citation of Gaussian 09, discussion of different calculation methods, energy surfaces of neutral Rh-catalyzed Diels–Alder reaction of ene-diene substrates, energy surfaces of cationic Rh-catalyzed Diels–Alder reaction of substituted ene-diene substrates, energy surface calculated by the M06 method, computed energy surface in solution, calculated energies of thermal Diels–Alder reactions, IRC calculations, optimized Cartesian coordinates and energies. This material is available free of charge via the Internet at http://pubs.acs.org.

■ AUTHOR INFORMATION

Corresponding Author

*E-mail: yuzx@pku.edu.cn.

Notes

The authors declare no competing financial interest.

■ ACKNOWLEDGMENTS

We are indebted to the generous financial support from the Natural Science Foundation of China (21232001) and the National Basic Research Program of China-973 Program (2011CB808600).

■ REFERENCES

(1) (a) Brieger, G.; Bennett, J. N. *Chem. Rev.* **1980**, *80*, 63. (b) Kagan, H. B.; Riant, O. *Chem. Rev.* **1992**, *92*, 1007. (c) Winkler, J. D. *Chem. Rev.* **1996**, *96*, 167. (d) Carmona, D.; Pilar Lamata, M.; Oro, L. A. *Coord. Chem. Rev.* **2000**, *200–202*, 717. (e) Nicolaou, K. C.; Snyder, S. A.; Montagnon, T.; Vassilikogiannakis, G. *Angew. Chem., Int. Ed.* **2002**, *41*, 1668. (f) Takao, K.-i.; Munakata, R.; Tadano, K.-i. *Chem. Rev.* **2005**, *105*, 4779. (g) Jiang, X.; Wang, R. *Chem. Rev.* **2013**, *113*, 5515.

(2) (a) Fleming, I. *Frontier Orbitals and Organic Chemical Reactions*; Wiley: New York, 1976. (b) Gilchrist, T. L.; Storr, R. C. *Organic Reactions and Orbital Symmetry*, 2nd ed.; Cambridge University Press: Cambridge, UK, 1971. (c) Fukui, K. *Acc. Chem. Res.* **1971**, *4*, 57. (d) Fukui, K. *Theory of Orientation and Stereoselection*; Springer-Verlag: Berlin, 1975.
(3) Pindur, U.; Lutz, G.; Otto, C. *Chem. Rev.* **1993**, *93*, 741.
(4) (a) Ciganik, E. *Org. React.* **1984**, *32*, 1. (b) Sauer, J. *Angew. Chem., Int. Ed. Engl.* **1966**, *5*, 211. (c) Fallis, A. G. *Can. J. Chem.* **1984**, *62*, 183. (d) Murakami, M.; Ubukata, M.; Itami, K.; Ito, Y. *Angew. Chem., Int. Ed.* **1998**, *37*, 2248.
(5) (a) Houk, K. N.; Li, Y.; Evanseck, J. D. *Angew. Chem., Int. Ed. Engl.* **1992**, *31*, 682. (b) Goldstein, E.; Beno, B.; Houk, K. N. *J. Am. Chem. Soc.* **1996**, *118*, 6036.
(6) (a) Li, Y.; Houk, K. N. *J. Am. Chem. Soc.* **1993**, *115*, 7478. (b) Froese, R. D. J.; Coxon, J. M.; West, S. C.; Morokuma, K. *J. Org. Chem.* **1997**, *62*, 6991.
(7) (a) Lautens, M.; Klute, W.; Tam, W. *Chem. Rev.* **1996**, *96*, 49. (b) Carmona, D.; Lamata, M. P.; Oro, L. A. *Coord. Chem. Rev.* **2000**, *200*, 717.
(8) Mörschel, P.; Janikowski, J.; Hilt, G.; Frenking, G. *J. Am. Chem. Soc.* **2008**, *130*, 8952.
(9) (a) Carbonaro, A.; Greco, A.; Dall'Asta, G. *J. Org. Chem.* **1968**, *33*, 3948. (b) tom Dieck, H.; Diercks, R. *Angew. Chem., Int. Ed. Engl.* **1983**, *22*, 778. (c) Wender, P. A.; Jenkins, T. E. *J. Am. Chem. Soc.* **1989**, *111*, 6432. (d) Wender, P. A.; Jenkins, T. E.; Suzuki, S. *J. Am. Chem. Soc.* **1995**, *117*, 1843. (e) Wender, P. A.; Smith, T. E. *J. Org. Chem.* **1996**, *61*, 824. (f) Murakami, M.; Itami, K.; Ito, Y. *J. Am. Chem. Soc.* **1997**, *119*, 7163. (g) Wender, P. A.; Smith, T. E. *Tetrahedron* **1998**, *54*, 1255. (h) Hilt, G.; Janikowski, J.; Hess, W. *Angew. Chem., Int. Ed.* **2006**, *45*, 5204. (i) Fürstner, A.; Stimson, C. C. *Angew. Chem., Int. Ed.* **2007**, *46*, 8845.
(10) Robinson, J. E. In *Modern Rhodium-Catalyzed Organic Reactions*; Evans, P. A., Ed.; Wiley-VCH Verlag GmbH & Co. KGaA: Weinheim, Germany, 2005; p 241.
(11) Matsuda, I.; Shibata, M.; Sato, S.; Izumi, Y. *Tetrahedron Lett.* **1987**, *28*, 3361.
(12) Paik, S.-J.; Son, S. U.; Chung, Y. K. *Org. Lett.* **1999**, *1*, 2045.
(13) (a) Jolly, R. S.; Luedtke, G.; Sheehan, D.; Livinghouse, T. *J. Am. Chem. Soc.* **1990**, *112*, 4965. (b) O'Mahony, D. J. R.; Belanger, D. B.; Livinghouse, T. *Org. Biomol. Chem.* **2003**, *1*, 2038.
(14) (a) Gilbertson, S. R.; Hoge, G. S. *Tetrahedron Lett.* **1998**, *39*, 2075. (b) O'Mahony, D. J. R.; Belanger, D. B.; Livinghouse, T. *Synlett* **1998**, *1998*, 443. (c) Richardson, B. M.; Day, C. S.; Welker, M. E. *J. Organomet. Chem.* **1999**, *577*, 120. (d) Wang, B.; Cao, P.; Zhang, X. *Tetrahedron Lett.* **2000**, *41*, 8041. (e) Motoda, D.; Kinoshita, H.; Shinokubo, H.; Oshima, K. *Angew. Chem., Int. Ed.* **2004**, *43*, 1860. (f) Lee, S. I.; Park, S. Y.; Park, J. H.; Jung, I. G.; Choi, S. Y.; Chung, Y. K.; Lee, B. Y. *J. Org. Chem.* **2005**, *71*, 91. (g) Yoo, W.-J.; Allen, A.; Villeneuve, K.; Tam, W. *Org. Lett.* **2005**, *7*, 5853. (h) Saito, A.; Ono, T.; Takahashi, A.; Taguchi, T.; Hanzawa, Y. *Tetrahedron Lett.* **2006**, *47*, 891.
(15) Sato, Y.; Oonishi, Y.; Mori, M. *Organometallics* **2002**, *22*, 30.
(16) (a) McKinstry, L.; Livinghouse, T. *Tetrahedron* **1994**, *50*, 6145. (b) Gilbertson, S. R.; Hoge, G. S.; Genov, D. G. *J. Org. Chem.* **1998**, *63*, 10077. (c) Davies, D. L.; Fawcett, J.; Garratt, S. A.; Russell, D. R. *Dalton. Trans.* **2004**, 3629. (d) Aikawa, K.; Akutagawa, S.; Mikami, K. *J. Am. Chem. Soc.* **2006**, *128*, 12648. (e) Shibata, T.; Fujiwara, D.; Endo, K. *Org. Biomol. Chem.* **2008**, *6*, 464. (f) Falk, A.; Fiebig, L.; Neudörfl, J.-M.; Adler, A.; Schmalz, H.-G. *Adv. Synth. Catal.* **2011**, *353*, 3357.
(17) Frisch, M. J.; et al. *Gaussian 09*, revision A.02; Gaussian, Inc.: Wallingford, CT, 2010.
(18) Parr, R. G.; Yang, W. *Density-Functional Theory of Atoms and Molecules*; Oxford University Press: Oxford, UK, 1989.
(19) (a) Lee, C.; Yang, W.; Parr, R. G. *Phys. Rev. B* **1988**, *37*, 785. (b) Becke, A. D. *J. Chem. Phys.* **1993**, *98*, 5648.
(20) Hehre, W. J.; Radom, L.; Schleyer, P. v. R.; Pople, J. A. *Ab Initio Molecular Orbital Theory*; Wiley: New York, 1986.
(21) Dunning, T. H., Jr.; Hay, P. J. In *Modern Theoretical Chemistry*; Schaefer, H. F., III, Ed.; Plenum Press: New York, 1977; pp 1−28.
(22) (a) Yu, Z.-X.; Wender, P. A.; Houk, K. N. *J. Am. Chem. Soc.* **2004**, *126*, 9154. (b) Liu, P.; Cheong, P. H.-Y.; Yu, Z.-X.; Wender, P. A.; Houk, K. N. *Angew. Chem., Int. Ed.* **2008**, *47*, 3939. (c) Yu, Z.-X.; Cheong, P. H.-Y.; Liu, P.; Legault, C. Y.; Wender, P. A.; Houk, K. N. *J. Am. Chem. Soc.* **2008**, *130*, 2378. (d) Jiao, L.; Lin, M.; Yu, Z.-X. *J. Am. Chem. Soc.* **2010**, *133*, 447. (e) Liu, P.; Sirois, L. E.; Cheong, P. H.-Y.; Yu, Z.-X.; Hartung, I. V.; Rieck, H.; Wender, P. A.; Houk, K. N. *J. Am. Chem. Soc.* **2010**, *132*, 10127. (f) Xu, X.; Liu, P.; Lesser, A.; Sirois, L. E.; Wender, P. A.; Houk, K. N. *J. Am. Chem. Soc.* **2012**, *134*, 11012.
(23) (a) Gonzalez, C.; Schlegel, H. B. *J. Chem. Phys.* **1989**, *90*, 2154. (b) Gonzalez, C.; Schlegel, H. B. *J. Phys. Chem.* **1990**, *94*, 5523.
(24) Legault, C. Y. *CYLView*, 1.0b; Université de Sherbrooke: Sherbrooke, Québec, Canada, 2009 (http://www.cylview.org).
(25) Bondi, A. *J. Phys. Chem.* **1964**, *68*, 441.